TOWARD A RAYLEIGH WAVE ATTENUATION MODEL FOR EURASIA AND CALIBRATING A NEW M_S FORMULA

Xiaoning (David) Yang[1], Anthony R. Lowry[2], Anatoli L. Levshin[2] and Michael H. Ritzwoller[2]

[1]Los Alamos National Laboratory, [2]University of Colorado at Boulder

Sponsored by National Nuclear Security Administration
Office of Nonproliferation Research and Engineering
Office of Defense Nuclear Nonproliferation

Contract No. [1]W-7405-ENG-36, [2]DE-FC52-05NA26608

ABSTRACT

We are characterizing Rayleigh wave attenuation for Eurasia using tomographic inversion of surface-wave amplitude data. These attenuation models will be used to calibrate the regional surface-wave magnitude scale and to extend the teleseismic M_s-m_b event discriminant to regional distances. Our research is based on the successful proof-of-concept study conducted by the LANL researchers to develop a 20s Rayleigh wave attenuation model for central and southeastern Asia. In order to minimize amplitude measurement errors caused by multipathing, focusing, and source uncertainty, LANL designed a measurement tool incorporating the phase-match filtering technique. The Surface Wave Amplitude Measurement TOOL (SWAMTOOL) proved effective in making reliable surface-wave amplitude measurements. A two-step inversion technique was employed using both two-station amplitude ratios and single-station amplitudes to better constrain the attenuation model.

In this study, we are developing shorter-period (10 – 18s) attenuation models for Eurasia covering geographical regions that increase in extent with period. At regional distances, the new M_s scale will most likely be measured at shorter periods and therefore requires shorter-period attenuation corrections. In order to make SWAMTOOL more suitable for measuring amplitudes at various periods more accurately, we have made modifications to improve its functionality. In addition to the existing ability of the tool to perform phase-match filtering and source parameter analysis, we added back-azimuth calculation using a cross-correlation technique. By comparing calculated back-azimuth with great-circle back-azimuth, we can assess whether the surface wave traveled along the great-circle path and, if not, the path deviation from the great circle. This information will help us to better identify the primary surface-wave arrival and better constrain the quality of the measurements. We also included pre-signal noise measurement in the tool. The noise level is used to identify the useful frequency band within which amplitude measurements have adequate signal-to-noise ratio.

We currently are collecting both two-station and single station waveform data for measurement. We will collect data both from permanent broadband and long-period stations in the region and from temporary PASSCAL deployments to improve data coverage, particularly at shorter periods.

OBJECTIVES

The objectives of the study are 1) to develop short-period (10 – 18s), two-dimensional (2-D) Rayleigh-wave attenuation models for Eurasia along with associated uncertainty statistics through a tomographic approach, and 2) to calibrate Russell's (2004) M_s formula with these models for the same region.

RESEARCH ACCOMPLISHED

In order to apply M_s-m_b discriminant to regional-distance monitoring, modified M_s formula using shorter-period (< 20) surface wave amplitudes is required (Marshall and Basham, 1970; Russell, 2004). Because shorter-period surface waves are sensitive to the Earth's crust, the strong lateral material-property heterogeneity of the crust could result in large surface-wave amplitude scatter due to lateral attenuation variations. To reduce this scatter, we are developing short-period (10 – 18s) 2-D surface-wave attenuation models for Eurasia through tomography, which can be used to account for 2-D path attenuation effects in regional M_s calculations.

Surface Wave Measurement TOOL (SWAMTOOL)

The accuracy of surface-wave attenuation measurements are affected by uncertainties in source-parameter estimates and site responses, and by medium elastic effects, with medium elastic effects such as multipathing, focusing, defocusing and off-great-circle paths being one of the principle sources of error (Mitchell, 1995; Selby and Woodhouse, 2000). As part of a previous 20s surface-wave attenuation study, LANL researchers designed a Surface Wave Amplitude Measurement TOOL (SWAMTOOL) to address some of these uncertainties (Yang et al., 2004). The measurement tool makes use of recently developed surface-wave group velocity models (Ritzwoller and Levshin, 1998; Levshin and Ritzwoller, 2003; Stevens et al., 2001; Levshin et al., 2003) to construct phase-matched filters (Herrin and Goforth, 1977) and applies these path-specific filters to the data before making amplitude measurements. The filtering process, along with the analysis of theoretical source radiation and spectra that is also part of the measurement tool, effectively reduced the bias caused by multipathing and focusing (Yang et al*.,* 2004). We will use SWAMTOOL to make surface-wave amplitude measurements for this study.

To improve the functionality of SWAMTOOL, we have made several modifications to the tool. We added back-azimuth calculations to the tool using a cross-correlation technique (Chael, 1997). Vertical-component seismogram is first Hilbert transformed to shift its phase by 90 degrees and then correlated with radial components for different azimuths between 0 and 360 degrees. The azimuth at which the maximum correlation is obtained is designated as the measured back-azimuth. This azimuth is then compared with great-circle back-azimuth to evaluate the path direction of the surface wave. The back-azimuth information will help us better identify the primary surface-wave arrival and better constrain the quality of the measurements. For example, we can use back-azimuth calculations to differentiate incoming directions of successive surface wave packets and therefore, facilitate the identification of the primary surface-wave arrival.

We also added pre-signal noise measurement in SWAMTOOL. The noise level is used to identify the useful frequency band within which amplitude measurements have adequate signal-to-noise ratios (S/N). Amplitude measurements with adequate S/N will be retained for the tomographic inversion.

Other miscellaneous modifications include adopting a larger-area map display and adding the ability to distinguish single-station amplitude measurement and two-station amplitude ratio measurement automatically. Figure 1 is a screen snapshot of the improved measurement tool. A detailed description of the tool is provided in the figure caption. The example shown in the figure illustrates the effectiveness of the measurement tool in identifying and removing multipathing and focusing effects. It also shows the use of back-azimuth calculations in aiding the differentiation of the primary arrival from the multipathed arrival. If we move the cross-correlation window to bracket the second pulse in the cross-correlation, the difference between measured back-azimuth and great-circle back-azimuth changes from -7 degrees to -23 degrees, indicating a more deviated path for the second wave packet.

Surface wave data collection

We are currently collecting surface-wave waveform data to prepare for amplitude measurements. In the first stage of data collection we have concentrated on events that occurred in and around Eurasia through 2000-2004.

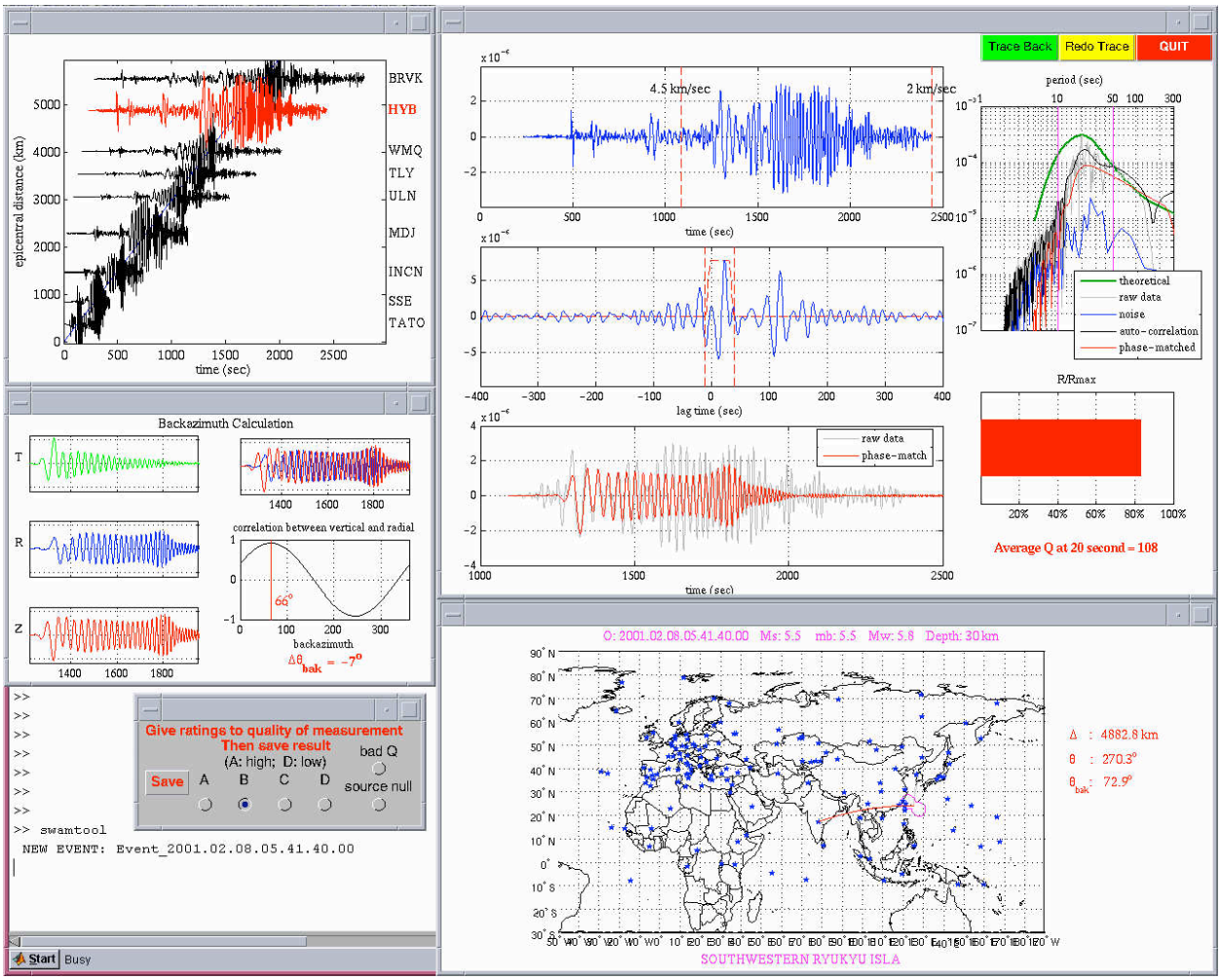

Figure 1. A snapshot of SWAMTOOL. In the upper-right window, the top-left plot shows the original seismogram. Crosscorrelation between the seismogram and the phase-matched filter for this path is plotted in the middle along with a window (red dashed line) isolating the primary arrival. The crosscorrelation shows a clear second arrival indicating multipathing. The lower figure on the left in this window shows the phase-match filtered seismogram (red) and the original seismogram (gray). The plot on the upper right of the window shows the theoretical source spectrum, the original data spectrum, the smoothed data spectrum through auto-correlation, the phase-match filtered data spectrum and the noise spectrum. The phase-match filtered spectrum is smooth and has a similar shape as the theoretical spectrum. Average attenuation at 20s for this path is calculated and displayed at the lower-right corner of this window. The lower-right window displays the map of the study region. The theoretical source radiation pattern and the path for this trace are plotted for the purpose of evaluating whether the path is in a source radiation null direction. A quantitative estimate is displayed in the upper-right window where the ratio between the amplitude of radiation in the path direction to the maximum amplitude is depicted as a percentage bar. Various source and path parameters are also displayed in the map window. Record section for this event is plotted in the upper-left window. The trace being analyzed is highlighted. Below the record-section window, results of back-azimuth calculation are displayed. In this window, different components of the data are plotted. The radial and vertical components are overlapped to assess their phase relationship. Comparison between measured back-azimuth and great-circle back-azimuth is displayed as the difference between the two azimuths. Finally, the analyst has an opportunity to assign a quality value to the measurement based on the information displayed on the screen.

We selected 486 events from the Harvard CMT Catalog (http://www.seismology.harvard.edu/CMTsearch.html) with $7.5 \geq M_s \geq 5.0$ inside the region from 10°S to 90°N and from 0°E to 160°E, and with the source depths less than 50 km. The map with the event distribution is shown in Figure 2.

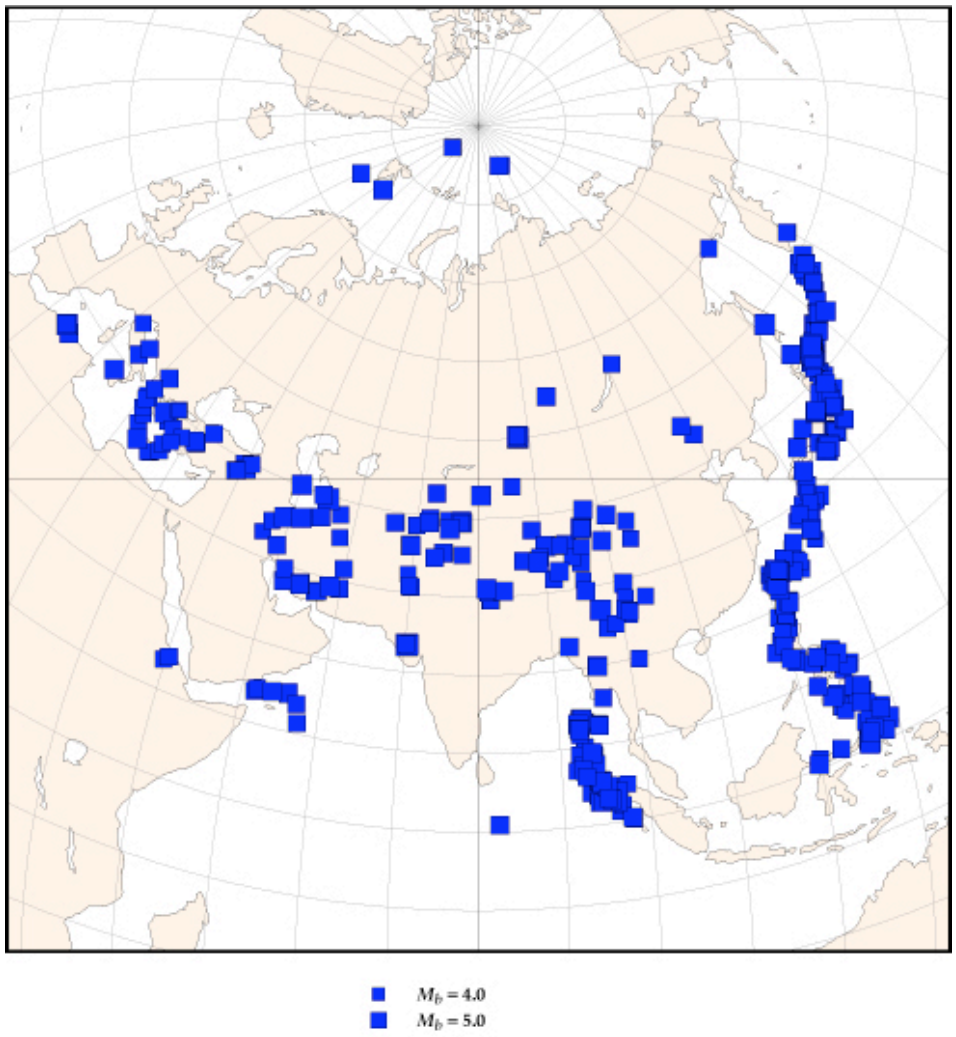

Figure 2. Events selected for first-stage surface-wave data collection.

Several global and regional broadband networks have existed in Eurasia during the considered time interval. These include Global Seismographic Network (GSN), International Monitoring System (IMS), GEOSCOPE, GEOFON, Mediterranean Seismic Network (MEDNET), China Seismological Digital Network (CDSN), Kyrgyz Seismic Network (KNET), Kazakhstan Seismic Network (KAZNET), and others. There have also been many temporary network deployments in the region including close to 10 PASSCAL projects. Figure 3 shows the distribution of stations belonging to different networks across the region. Waveforms from these stations are available through IRIS DMC.

The waveform collection and preliminary waveform evaluation are now in progress. In addition to the events that we have selected, we also plan to collect waveforms for the events that occurred in 2005, and if necessary, for smaller events between 2000 and 2005 with $M_s \geq 4.5$ or $m_b \geq 5.0$ if M_s is absent.

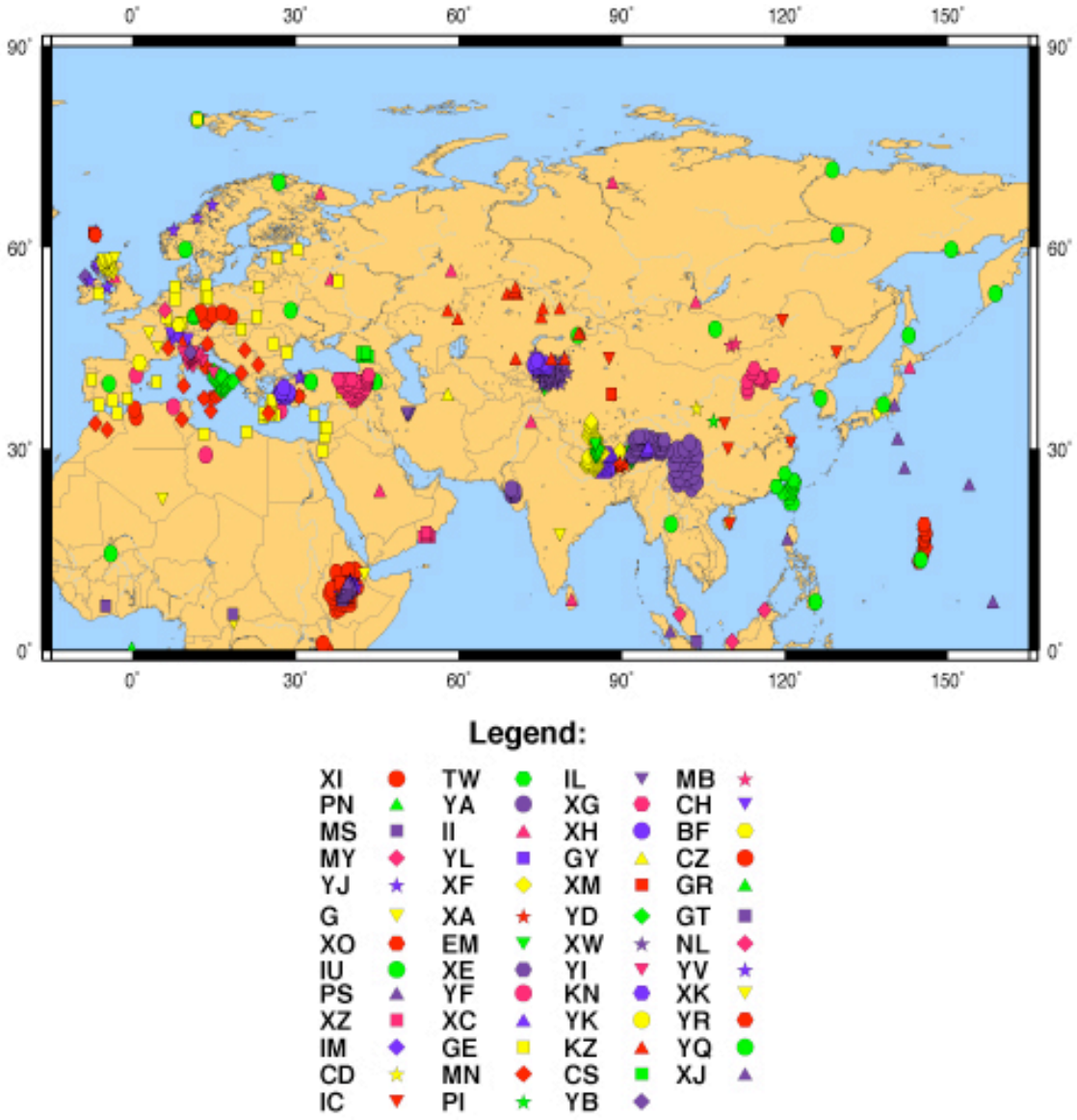

Figure 3. Station distribution for the data collection.

Calibrating Russell's M_s formula for Eurasia

The M_s formula proposed by Russell (2004) represents the latest development in regional surface-wave magnitude research. This formula requires amplitudes measured at variable periods as well as regional calibration for its parameterization. One approach of calculating magnitudes at variable periods is to make a suite of amplitude measurements at all periods within a frequency band and select the measurement that gives the maximum magnitude (Bonner et al., 2004). An alternative would be to calibrate, for a particular region, e.g., Eurasia, the optimum periods at which surface wave amplitudes yield the maximum magnitudes. These optimum periods will depend on variables such as path length, source size, location and depth, and the medium structure along the path. The mapping of the optimum periods as a function of these variables will provide important background information for M_s regionalization.

As the first step to investigate the regionalization of Russell's M_s formula for Eurasia, we measured the periods at which surface waves have the largest amplitudes from the amplitude dataset that LANL measured for the Asia 20s surface-wave attenuation study (Yang et al., 2004). Figure 4 plots the period of the maximum surface-wave

amplitude as a function of source-receiver distance. The data show a large scatter reflecting the different source and path effects. There is also a tendency of increasing periods as path lengths become longer. Nevertheless, the majority of the periods are below 20 seconds even for paths as long as close to 6000 km. Another observation is that even for the shortest paths considered, the periods are rarely below 10 seconds.

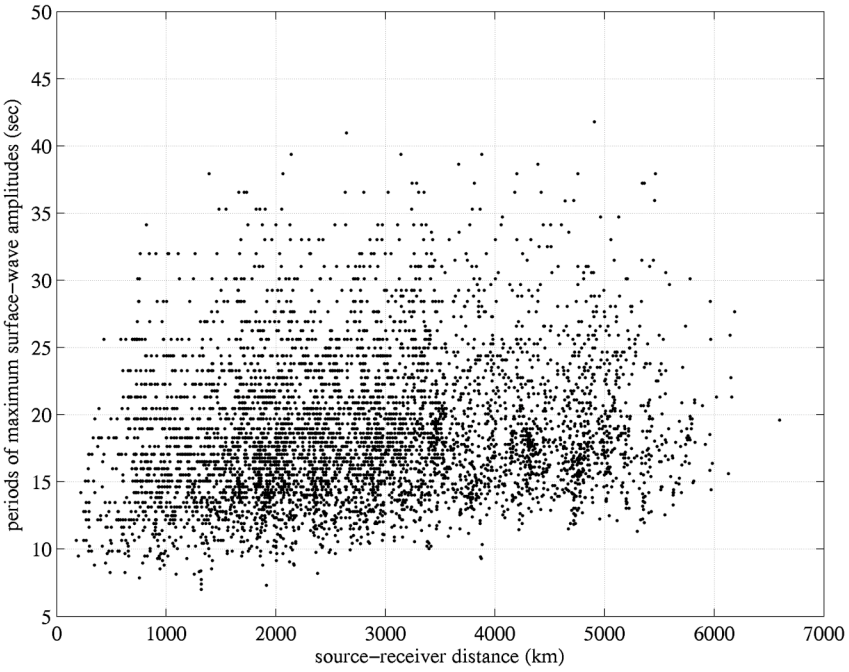

Figure 4. Periods of maximum surface-wave amplitudes from a data set of approximately 5200 measurements for the region of central and southeastern Asia.

CONCLUSIONS AND RECOMMENDATIONS

We have finished modification of the Surface Wave Amplitude Measurement Tool to include the back-azimuth calculation and noise measurement. This tool will be used for the short-period surface-wave amplitude and amplitude ratio analysis and measurement. We have selected 486 events with CMT solutions for the study region to make waveform data collection.

ACKNOWLEDGEMENTS

Surface-wave waveform data were obtained through IRIS DMC. Harvard CMT Catalog was used in the study. We thank Dr. Misha Barmin of CU-Boulder for his help in data collection and computer program setup. Review by Dr. Richard Stead of LANL is appreciated.

REFERENCES

Bonner, J. L., D. T. Reiter, D. G. Harkrider, and S. A. Russell (2004). Development of a Time-Domain, Variable-Period Surface Wave Magnitude Measurement Procedure for Application at Regional Distances, in *Proceedings of the 26th Seismic Research Review: Trends in Nuclear Explosion Monitoring*, Orlando, FL (Sept. 21–23, 2004), LA-UR-045801, Vol. 1: pp. 377-386.

Chael, E. P. (1997). An Automated Rayleigh-Wave Detection Algorithm, *Bull. Seism. Soc. Am.* 87: 157-163.

Herrin, E. E. and T. T. Goforth (1977). Phase-Matched Filters: Application to the Study of Rayleigh Waves, *Bull. Seism. Soc. Am.* 67: 1259-1275.

Levshin, A. L. and M. H. Ritzwoller (2003). Discrimination, Detection, Depth, Location, and Wave Propagation Studies Using Intermediate Period Surface Waves in the Middle East, Central Asia, and the Far East, Technical Report DTRA-TR-01-28, Defense Threat Reduction Agency, Fort Belvoir, Virginia, 120 pp..

Levshin, A. L., J. L. Stevens, M. H. Ritzwoller, D. A. Adams and G. E. Baker (2003). Improvement of Detection and Discrimination Using Short Period (7s-15s) Surface Waves in W. China, N. India, Pakistan and Environs, Final Report, submitted to Defense Threat Reduction Agency, Fort Belvoir, Virginia, 49 pp..

Marshall, P. D. and P. W. Basham (1972). Discrimination Between Earthquakes and Underground Explosions Employing an Improved M_s Scale, *Geophys. J. R. astr. Soc.* 28: 431-458.

Mitchell, B. J. (1995). Anelastic Structure and Evolution of the Continental Crust and Upper Mantle from Seismic Surface Wave Attenuation, *Rev. Geophys.* 33: 441-462.

Ritzwoller, M. H. and A. L. Levshin (1998). Eurasian Surface Wave Tomography: Group Velocities, *J. Geophys. Res*. 103: 4839-4878.

Russell, D. R. (2004). Theoretical Analysis of Narrow-Band Surface Wave Magnitudes, Technical Report, AFTAC-TR-04-004, Air Force Technical Applications Center, 36 pp..

Selby, N. D. and J. H. Woodhouse (2000). Controls on Rayleigh Wave Amplitudes: Attenuation and Focusing, *Geophys. J. Int*. 142: 933-940.

Stevens, J. L., D. A. Adams and G. E. Baker (2001). Improved Surface Wave Detection and Measurement Using Phase-Matched Filtering with a Global One-Degree Dispersion Model, in *Proceedings of the 23rd Seismic Research Review: Worldwide Monitoring of Nuclear Explosions*, LA-UR-01-4454, Vol. 1: pp. 420-430.

Yang, X., S. R. Taylor and H. J. Patton (2004). The 20-S Rayleigh Wave Attenuation Tomography for Central and Southeastern Asia, *J. Geophys. Res.* 109, B12304, doi:10.1029/2004JB003193.